Applied and Environmental Microbiology

A class IV adenylate cyclase CyaB is required for capsule polysaccharide production and biofilm formation in *Vibrio parahaemolyticus*

Regmi, A., J.G. Tague, K. Boas Lichty, and E.F. Boyd*

Department of Biological Sciences, University of Delaware, Newark, DE 19716

Corresponding author*

E. Fidelma Boyd

Department of Biological Sciences

341 Wolf Hall, University of Delaware

Newark, DE 19716

Phone: (302) 831-1088. Fax: (302) 831-2281 Email: fboyd@udel.edu

ABSTRACT

CRP (cyclic AMP receptor protein), encoded by *crp*, is a global regulator that is activated by cAMP (cyclic AMP), a second messenger synthesized by a class I adenylate cyclase (AC-I) encoded by *cyaA* in *Escherichia coli*. cAMP-CRP is required for growth on non-preferred carbon sources and is a global regulator. We constructed in-frame non-polar deletions of the *crp* and *cyaA* homologs in *Vibrio parahaemolyticus* and found that the Δ*crp* mutant did not grow in minimal media supplemented with non-preferred carbon sources, but the Δ*cyaA* mutant grew similar to wild type. Bioinformatics analysis of the *V. parahaemolyticus* genome identified a 181 amino acid protein annotated as a class IV adenylate cyclase (AC-IV) named CyaB, a member of the CYTH protein superfamily. AC-IV phylogeny showed CyaB was present in Gamma- and Alpha-Proteobacteria as well as Planctomycete and Archaea. Only the bacterial CyaB proteins contained an N-terminal motif HFxxxExExK indicative of adenylyl cyclase activity. Both *V. parahaemolyticus cyaA* and *cyaB* genes functionally complemented an *E. coli* Δ*cyaA* mutant. The Δ*crp* and Δ*cyaB*/Δ*cyaA* mutants showed defects in growth on non-preferred carbon sources, and in swimming and swarming motility, indicating cAMP-CRP is an activator. The Δ*cyaA* and Δ*cyaB* single mutants had no defects in these phenotypes indicating AC-IV complements AC-I. Capsule polysaccharide and biofilm production assays showed significant defects in Δ*crp*, Δ*cyaB*/Δ*cyaA,* and the Δ*cyaB* mutant, whereas Δ*cyaA* behaved similar to wild type. This is consistent with a role of

44 cAMP-CRP as an activator of these phenotypes and establishes a cellular role for AC-IV
45 in capsule and biofilm formation, which to date has been unestablished.

46 **IMPORTANCE**

47 Here, we characterized the roles of CRP and CyaA in *V. parahaemolyticus,* showing
48 cAMP-CRP was an activator of metabolism, motility, capsule and biofilm formation.
49 These results are in contrast to cAMP-CRP in *V. cholerae,* which represses capsule and
50 biofilm formation. Previously, only an AC-I CyaA had been identified in *Vibrio* species.
51 Our data showed that an AC-IV CyaB homolog is present in *V. parahaemolyticus* and
52 was required for optimal growth. The data demonstrated that CyaB was essential for
53 capsule production and biofilm formation uncovering a physiological role of AC-IV in
54 bacteria. The data showed that the *cyaB* gene was widespread among *Vibrionaceae*
55 species and several other Gamma-Proteobacteria, but in general, its phylogenetic
56 distribution was limited. Our phylogenetic analysis also demonstrated that in some
57 species the *cyaB* gene was acquired by horizontal gene transfer.

58

59 **INTRODUCTION**

60 Carbon catabolite repression (CCR) is a global regulatory mechanism that represses
61 functions required for secondary carbon metabolism when a preferred carbon source is
62 present (1, 2). In *Escherichia coli,* CCR is mediated by several mechanisms such as the
63 regulation of the biosynthesis of catabolic enzymes, the inhibition of carbon transport,
64 and metabolic signaling (3, 4). Some of the major players involved in CCR are the global
65 regulator CRP (**c**AMP **R**eceptor **P**rotein), adenylate cyclase (AC), the signaling molecule
66 cAMP (3′,5′-cyclic AMP), and components of phosphoenolpyruvate:sugar
67 phosphotransferase system (PTS) transporters (1, 3-7). CRP functions as a homodimer,
68 activated by the second messenger cAMP and in *E. coli* cAMP-CRP is a global
69 transcriptional activator of non-preferred carbon genes in the absence of glucose (8-10).
70 In *E. coli*, CRP has an N-terminal cAMP binding domain (CBD; residues 1–136) and a C-
71 terminal helix turn helix DNA binding domain (DBD; residues 139–209) (11, 12). When
72 bound by cAMP, CRP undergoes a conformation change that allows the protein to
73 interact with target promoter regions at consensus sequences (13, 14).
74 When glucose is present, it is imported by the PTS transporter, resulting in
75 dephosphorylation of the EIIA component of PTS. $EIIA^{glc}$ inhibits non-preferred carbon
76 transporters, a mechanism known as inducer exclusion, independent of cAMP signaling
77 (2, 4, 15-17). When glucose is absent, $EIIA^{glc}$ is phosphorylated and $P{\sim}EIIA^{glc}$ activates
78 adenylate cyclase to produce cAMP (4, 18). However, growth on non-PTS carbon

79 sources, such as lactose, and in limited nitrogen and phosphorous conditions also have
80 reduced cAMP levels, indicating the presence of a catabolite modulating factor, which
81 Monod suggested in his last paper (19). Recent research showed that cAMP signals
82 were modulated by metabolic precursors such as α-ketoacids to control the allocation of
83 proteomic resources by a feedback system rather than carbon metabolism (20, 21).
84 There are six classes (I-VI) of adenylate cyclases (AC) based on primary amino
85 acid sequence, all with different catalytic mechanisms and structures, indicating
86 different evolutionary origins (22, 23). *Escherichia coli* and many other *Proteobacteria*
87 contain a single AC gene *cyaA*, which encodes a class I AC (AC-I). The 810 amino acid
88 CyaA protein has two functionally distinct domains, the N-terminal catalytic cyclase
89 domain and the C-terminal regulatory domain (11, 12, 24). Class II ACs (AC-II) are
90 comprised of bacterial toxins such as the exotoxin from *Bordetella pertussis* (25). The class
91 III ACs (AC-III) are the most diverse and widespread, and encompass adenylate
92 cyclases present in eukaryotes and prokaryotes (26). A structurally diverse AC was
93 identified in *Prevotella ruminicola* D31d and forms the sole representative of AC-V (27).
94 A class VI AC was described in *Rhizobium elti*, a 345 amino acid protein that was shown
95 to have cyclase activity by complementation of an *E. coli cyaA* deletion mutant (28).
96 Class IV AC (AC-IV) along with mammalian thiamine triphosphatases and
97 inorganic triphosphatases belong to the CYTH-like domain superfamily (29). CYTH
98 proteins are present in all three domains, Bacteria, Archaea and Eukaryota, and perform

99 a variety of functions (29). CYTH proteins contain a triphosphate tunnel metaloenzyme
100 (TTM) fold and act on triphosphorylated substrates with at least one divalent metal
101 cation required for catalysis. A hallmark of CYTH proteins is an N-terminal ExExK
102 motif (30). In bacteria, an AC-IV CyaB was initially described in *Aeromonas hydrophila,* a
103 small 181 amino acid protein with a single domain (31). The foundational work in *A.*
104 *hydrophila* indicated that *cyaB* was not expressed under standard growth conditions, but
105 *cyaB* did functionally complement an *E. coli cyaA* deletion mutant (31). A CyaB homolog
106 was also identified from *Yersinia pestis*, its crystal structure (2FJT) was determined and
107 showed to be very different from AC-I and AC-III enzymes. AC-IV formed a dimer like
108 AC-III, but with a distinct antiparallel eight-stranded barrel active site and could cyclize
109 both ATP and GTP (32-34). The physiological role of bacterial AC-IV was not
110 established. Archaea contain numerous proteins annotated as AC-IV, but cAMP
111 biosynthesis has not been shown for this domain (35). A recent study examining a
112 CYTH-like protein annotated as an AC-IV from the Crenarchaeote *Sulfolobus*
113 *acidocaldarius* showed that it had triphosphatase activity, but no adenylate cyclase
114 activity (35). Vogt and colleagues differentiated CYTH-like proteins (with phosphatase
115 activity) from AC-IV (with adenylyl cyclase activity) using sequence similarity network
116 analysis and functional studies (35). They suggested that a true AC-IV has an extended
117 N-terminal motif HFxxxxExExK and the absence of HF indicates a CYTH protein with
118 either thiamine triphosphatase (ThTPase) or inorganic triphosphatase activity (35).

119 In the present study, the function and activation of CRP in *V. parahaemolyticus*
120 was investigated for the first time. In-frame non-polar deletions of *crp* (VP2793) and
121 *cyaA* (VP2987) in *V. parahaemolyticus* RIMD2201633 were constructed and examined for
122 growth on various carbon sources. The Δ*crp* mutant grew on minimal medium M9 3%
123 NaCl supplemented with glucose (M9G) and was unable to grow on non-PTS carbon
124 sources, but the Δ*cyaA* mutant grew similar to wild type. This suggested the presence of
125 an additional uncharacterized AC in *V. parahaemolyticus*. Bioinformatics analysis
126 identified ORF VP1760 that encoded a putative AC-IV named CyaB. The phylogeny of
127 AC-IV among Bacteria and their closest orthologs in Archaea was examined to
128 determine its distribution and evolutionary history. To examine whether *cyaA* and *cyaB*
129 were both functional, an *E. coli* Δ*cyaA* mutant was functionally complemented with both
130 genes. Growth pattern analysis of the Δ*cyaB,* Δ*cyaA* and a double Δ*cyaB*/Δ*cyaA* mutants
131 on different carbon sources was also examined. Swimming and swarming motility
132 assays, capsule polysaccharide (CPS) production and biofilm formation assays were
133 performed to determine whether cAMP-CRP played a role in these important
134 phenotypes.

135 **RESULTS**

136 **CRP is an essential regulator in *V. parahaemolyticus.***

137 cAMP-CRP is a global regulator of nutrient transport and metabolism in many bacterial
138 species (13, 36-40). Homologs of CRP and CyaA are present in *V. parahaemolyticus*, ORF

139 VP2793 and VP2987, respectively (**Fig. S1**). The CRP and CyaA proteins of *V.*
140 *parahaemolyticus* shared 98% and 82% amino acid identity respectively to homologs in *V.*
141 *cholerae*. The genome context of both genes is conserved across *V. parahaemolyticus*, *V.*
142 *cholerae,* and *E. coli* (**Fig. S1**). To begin to investigate the physiological role of CRP in *V.*
143 *parahaemolyticus,* we first constructed an in-frame non-polar deletion of *crp* (VP2793)
144 and *cyaA* (VP2987) in *V. parahaemolyticus* RIMD2210633. The Δ*crp* mutant displayed a
145 small colony morphology on LB supplemented with 3% NaCl (LBS) plates **(Fig. S2A)**.
146 Growth pattern analysis in LBS broth and M9S D-glucose broth demonstrated that the
147 Δ*crp* strain had a growth defect **(Fig. 1A**-**B**). Next, we examined the Δ*cyaA* mutant,
148 expecting a phenotype similar to the Δ*crp* mutant, as shown in *E. coli* and *V. cholerae*
149 Δ*cyaA* mutants. However, growth of Δ*cyaA* on LBS plates gave identical colony
150 morphology to wild type (**Fig. S2A)** and similarly in LBS and M9 supplemented with
151 3% NaCl (M9S) and D-glucose broth, Δ*cyaA* presented a similar pattern to wild type
152 (**Fig. 1A**-**B**). In addition, growth in alternative carbon sources, M9S supplemented with
153 L-arabinose, L- ribose, or D-gluconate, showed the Δ*crp* strain was defective, but the
154 Δ*cyaA* mutant grew similar to wild type (**Fig 2A-C**). These data demonstrate that CRP is
155 required for catabolism of alternative carbon sources similar to *V. cholerae*, but that *V.*
156 *parahaemolyticus* contained an additional uncharacterized adenylate cyclase that can
157 synthesize cAMP in the absence of *cyaA* to activate CRP. Alternatively, CRP could be

158 acting independently of cAMP, but given its high homology to CRP from *V. cholerae* this
159 is less likely.

160 **Identification of a class IV adenylate cyclase (AC-IV) CyaB in *V. parahaemolyticus*.**

161 BLASTP analysis using CyaA (VP2987) as a seed to search the *V. parahaemolyticus*
162 RIMD2210633 genome, only hit to itself, indicating no other homolog of AC-I was
163 present. Then, a search of the *V. parahaemolyticus* genome for adenylate cyclase classes
164 AC-II using locus WP_080378568 from *Bordetella pertussis*, AC-III using locus PWU33926
165 from *Pseudomonas aeruginosa*, and AC-IV using locus UNB56521 from *A. hydrophila,* was
166 performed. In addition, ten AC proteins (loci Rv0386, Rv1264, Rv1318c, Rv1319c,
167 Rv1320c, Rv1625c, Rv1647, Rv1900c, Rv2212, Rv3645) encompassing AC-II and AC-III
168 from *Mycobacterium tuberculosis* that were shown to have activity were also used as
169 seeds. These searches identified a homolog of AC-IV from *A. hydrophila* named CyaB.
170 No additional adenylate cyclases were identified in *V. parahaemolyticus* RIMD2210633.
171 The 181 amino acid CyaB protein lacked transmembrane domains and signal peptide
172 cleavage sites. CyaB contained only one domain and unlike AC-I, AC-II and AC-III does
173 not contain any regulatory or signaling domains. CyaB shared 56% amino acid identity
174 with CyaB of *A. hydrophila* and 45% amino acid identity with CyaB from *Y. pestis*. CyaB
175 from both *A. hydrophila* and *Y. pestis* were shown to have AC activity generating cAMP,
176 however a physiological role was not established (31-34). In *V. parahaemolyticus, cyaB* is
177 encoded on the negative strand upstream of VP1761, which encoded a DUF962-domain

178 hypothetical protein separate by an intergenic region of 88-bp. The AC-IV CyaB protein
179 has been structurally characterized in *Y. pestis* (2FJT and 3NOY) and a crystal structure
180 is also available for VP1760 from *V. parahaemolyticus* (2ACA) (32-34). Comparison of *Y.*
181 *pestis* and *V. parahaemolyticus* primary sequence and crystal structures shows they are
182 highly similar with active sites conserved between the proteins (**Fig. S3**). The primary
183 sequence of all three bacterial sequences contained the N-terminal conserved
184 HFxxxxExExK motif and the archaea sequences contained the shorter ExExK motif (**Fig.**
185 **S3**).

186 **Distribution and phylogenetic analysis of AC-IV among Bacteria**.

187 Using *cyaB* (VP1760) as a seed using BLAST analysis, we examined the distribution
188 among nearly 18,000 members of the family *Vibrionaceae* in the NCBI genome database.
189 The *cyaB* gene was present in all characterized *V. parahaemolyticus* strains and in many
190 members of the Harveyi clade, to which *V. parahaemolyticus* belongs, including *V.*
191 *campbellii, V. harveyi, V. jasicida, V. owensii,* and *V. rotiferanus* (**Fig. 3**). The CyaB proteins
192 in these species showed ~70% amino acid identity with CyaB from *V. parahaemolyticus,*
193 as compared to ~95% amino acid identity among the CyaA proteins. On the *cyaB* gene
194 tree, within the Harveyi clade, species formed two divergent branches; one branch
195 representing *V. parahaemolyticus* strains and the second branch containing the remaining
196 species. This suggests that *cyaB* in *V. parahaemolyticus* has diverged significantly from
197 *cyaB* in the other Harveyi clade species. Interestingly, CyaB was absent from most *V.*

198 *alginolyticus* strains, a species closely related to *V. parahaemolyticus*. Our analysis did
199 identify a *V. alginolyticus* strain that contained a *cyaB* gene on a plasmid that clustered
200 within the same group as *cyaB* present on a plasmid in *V. coralliilyticus* indicating that
201 *cyaB* was acquired by horizontal gene transfer in these species (**Fig. 3**). The *cyaB* gene
202 was present in ~35 *V. cholerae* strains (from a total of 1,700 genomes in the NCBI
203 database) and two strains of its sister species *V. metoecus* from a total of 30 genomes,
204 which clustered together on the tree. The *cyaB* gene from species within the genera
205 *Aliivibrio* and most *Photobacterium* formed separate divergent branches from *cyaB* in
206 *Vibrio* species (**Fig. 3**). However, *cyaB* from five *Photobacterium* species clustered within
207 *Vibrio* clades suggesting that these *Photobacterium* species acquired a copy of the *cyaB*
208 gene from *Vibrio*, indicating horizontal gene transfer (**Fig. 3**). Comparison of CyaA
209 phylogeny with the CyaB phylogeny from the same set of species also demonstrated
210 additional instances of horizontal transfer among species shown by the non-congruency
211 of the branching patterns for several CyaB proteins (**Fig. S4**).
212 Next, we examined the distribution and phylogeny of AC-IV among Bacteria and
213 Archaea genomes in the NCBI genome database (**Fig. 4**). This analysis showed that AC-
214 IV were present predominantly among Gamma-Proteobacteria. CyaB from some species
215 belonging to the genera *Shewanella, Marinomonas, Psychromonas,* and *Morganella*
216 clustered closely with CyaB from *Vibrio* species. Species belonging to the genera
217 *Aeromonas, Yersinia, Brennia, Dickeya, Hafnia, Proteus Providencia,* and *Pectobacterium*

218 contained a copy of CyaB that branched along phylogeny lines indicating that CyaB is
219 ancestral to these lineages (**Fig. 4**). A handful of Alpha-Proteobacteria, *Cohaesibacter,*
220 *Hoeflea, Kangsaoukella, Maritalea, and Pseudovibrio,* also contained a CyaB homolog that
221 was annotated as AC-IV and these clustered together and branched distantly from
222 CyaB in Gamma-Proteobacteria (**Fig. 4**). Proteins showing greater than 25% amino acid
223 identity with greater than 90% query coverage to CyaB from *V. parahaemolyticus* were
224 present in Archaea and branched divergently from AC-IV homologs in Bacteria (**Fig. 4**).
225 Amino acid sequence comparisons followed by WebLogo analysis of Proteobacteria or
226 Archaea CyaB sequences was performed and generated sequence logos for the entire
227 protein in both groups to identify sequence conservation patterns (**Fig. S5 and S6**). In
228 this analysis, the previously identified AC-IV defining N-terminal motif HFxxxExExK
229 was present in all Gamma-Proteobacteria and Alpha-Proteobacteria sequences
230 examined in this study (**Fig. S5**). In contrast, CyaB representatives from Planctomycete
231 and Archaea contained the N-terminal motif ExExK, which was proposed to be present
232 in CYTH proteins with only phosphatase activity (**Fig. S6**) (35).

233 **AC-IV CyaB functionally complements an *E. coli cyaA* deletion mutant**.

234 To begin to determine whether CyaB has adenylate cyclase activity, we functionally
235 complemented an *E. coli* Δ*cyaA* mutant with the *cyaA* or *cyaB* gene from *V.*
236 *parahaemolyticus*. *E. coli* Δ*cyaA*, *E. coli* Δ*cyaA* pBBR*cyaB,* and *E. coli* Δ*cyaA* pBBR*cyaA* were
237 grown in M9S supplemented with glucose as a sole carbon source and all strains grew

238 similarly (**Fig. 5A**). Growth was examined in M9S supplemented with gluconate as a
239 sole carbon source. In this analysis, the growth defect of *E. coli* Δ*cyaA* was rescued in *E.*
240 *coli* Δ*cyaA* complemented with either pBBR*cyaA* or pBBR*cyaB* (**Fig. 5B)**.
241 To investigate the role of *cyaB* in *V. parahaemolyticus* physiology further, we
242 constructed a *cyaB* deletion mutant strain. We examined growth of wild type and the
243 Δ*cyaB* mutant on solid and in liquid media. The Δ*cyaB* mutant had similar colony
244 morphology to wild type on LBS plates (**Fig. S2A**) and showed identical growth
245 patterns in LBS broth to wild type **(Fig. 1A)**. However, when the Δ*cyaB* mutant was
246 grown overnight in M9S D-glucose and used to inoculate M9 supplemented with D-
247 glucose, a longer lag phase than wild type was observed, but a similar biomass was
248 reached **(Fig. 1B)**.
249 Next, we constructed a Δ*cyaB*/Δ*cyaA* double mutant strain by deleting *cyaA* from the
250 Δ*cyaB* background. The double mutant demonstrated small translucent colony
251 morphology on LBS similar to the colonies observed for Δ*crp* **(Fig. S2A and C)**.
252 Addition of cAMP to the media restored the large colony morphology for the double
253 mutant indicating that the defect was due to the absence of cAMP (**Fig. S2D**).
254 Interestingly, a glycerol stock of the double mutant when streaked on LBS plates
255 produced small translucent colonies as well as regular opaque colonies, suggesting
256 suppressor mutations were occurring (**Fig. S2B**). We did not observed this phenotype in
257 either of the single Δ*cyaA or* Δ*cyaB* mutants. In *V. cholerae,* which contains only an AC-I

258 CyaA, the Δ*cyaA* mutant reversion to wild-type phenotypes was also observed (41). For
259 our studies, small colonies were always used for phenotypic assays. The Δ*cyaB*/Δ*cyaA*
260 double mutant showed a growth defect on M9S D-glucose (**Fig. 1B**) and showed no
261 growth in M9 supplemented with L-arabinose, L-ribose, or D-gluconate **(Fig. 2A-C)**.
262 These growth assays were performed in M9S L-arabinose, L-ribose, or D-gluconate with
263 inoculum obtained after overnight growth in M9S D-glucose. These growth assays
264 showed that the Δ*cyaA* mutant grew similar to wild type, but the Δ*cyaB* mutant growth
265 curve showed a different slope (**Fig. 2**). In contrast, when mutants were grown
266 overnight in LBS and then inoculated into alternative carbon sources, Δ*cyaB* growth
267 curves showed a shorter lag phase and a significantly greater biomass than Δ*cyaA*,
268 which grew similar to wild type (**Fig. S7**). Analysis of the regulatory regions of both AC
269 genes identified putative CRP binding sites in the regulatory region of *cyaA,* but not in
270 the *cyaB* regulatory region (**Fig. S8**). These data suggest that *cyaA* is under CRP control
271 and that *cyaB* is not, and that CyaA and CyaB can complement each other.
272 **cAMP-CRP regulation of swimming and swarming motility**.
273 Unlike *V. cholerae* which only produces a polar flagellum, *V. parahaemolyticus* produces
274 both polar and lateral flagella required for swimming and swarming motility,
275 respectively, which are both activated by the sigma factor RpoN (42). To investigate the
276 role of CRP in *V. parahaemolyticus* motility, we conducted swimming assays and found
277 that the Δ*cyaA* and Δ*cyaB* mutants grew similar to wild type (**Fig. 6A**). The Δ*crp* and

278 Δ*cyaB*/Δ*cyaA* double mutants were defective in swimming compared to wild type, but
279 did not show a complete defect similar to the Δ*rpoN* mutant (**Fig. 6A**). Also, Δ*crp* and
280 Δ*cyaB*/Δ*cyaA* mutant showed a swarming defect as indicated by the absence of the
281 budding phenotype (**Fig. 6B**). The Δ*cyaA* and Δ*cyaB* mutants grew similar to wild type
282 producing typical budding swarming cells as previously shown for this species (**Fig.**
283 **6B**) (43-45). The WT, Δ*cyaA* and Δ*cyaB* swarming colonies were examined further to
284 show that the swarming colony structural differences were not due to mutants forming.
285 To accomplish this, different parts of the swarming colony were re-streaked onto
286 swarming plates and examined after 48 h at 30˚C, which again showed similar colony
287 morphologies to the original colonies (**Fig. S9**). Since Δ*crp* and Δ*cyaB*/*cyaA* both gave a
288 small colony morphology on swarming plates after 48 h of growth at 30˚C, we extended
289 the incubation time to 64 h at 30˚C to ensure no swarming motility occurred **(Fig. S10).**
290 Overall, the data demonstrate that cAMP-CRP is an activator of both swimming and
291 swarming motility in *V. parahaemolyticus*.

292 **cAMP-CRP and AC-IV CyaB are required for capsule and biofilm production.**

293 Capsule polysaccharide (CPS) is an important component of biofilm and is positively
294 controlled by the quorum sensing master regulator OpaR in *V. parahaemolyticus* (43, 44,
295 46-49). To determine whether CRP plays a role in CPS formation, we examined the Δ*crp*,
296 Δ*cyaA*, Δ*cyaB*, and Δ*cyaB*/*cyaA* mutants on HI medium containing Congo red dye and
297 $CaCl_2$. After incubation for 48 h at 30˚C, the wild type strain produced a rugose opaque

298 colony as did the Δ*cyaA* mutant, both indicatingf CPS production (**Fig. 7**). However, the
299 Δ*cyaB* mutant produced a smooth translucent colony as did the Δ*crp* and Δ*cyaB*/Δ*cyaA*
300 mutants indicating absence of CPS (**Fig. 7**). In biofilm assays, wild type and Δ*cyaA*
301 produced significant biofilm, whereas Δ*crp*, Δ*cyaB,* and Δ*cyaB*/Δ*cyaA* produced
302 significantly less biofilm compared to wild type (**Fig. 8**). Overall, these data
303 demonstrate that both CRP and CyaB, but not CyaA, are required for CPS and biofilm
304 production in *V. parahaemolyticus*. We functionally complemented a *V. parahaemolyticus*
305 Δ*cyaB* mutant with the *cyaB* gene on an expression vector and a biofilm assay was
306 performed. In this assay the wild type pBBREV (empty vector), Δ*cyaB* pBBREV, and
307 Δ*cyaB* pBBR*cyaB* were examined and the Δ*cyaB* pBBR*cyaB* complement showed
308 restoration of biofilm to wild type levels (**Fig. S11**).
309 Both Δ*crp* and Δ*opaR* deletion mutants have significant defects in capsule formation and
310 biofilm production. It was previously shown that OpaR is an activator of CPS binding
311 to the regulatory regions of the CpsA-K biosynthesis cluster and CPS regulators CspQ,
312 CpsR, and CpsS in *V. parahaemolyticus* BB22OP (50). We examined whether CRP and
313 OpaR interact to control CPS production. To accomplish this, functional complement
314 experiments of Δ*crp* and Δ*opaR* with either *crp* or *opaR* were performed. As controls,
315 both Δ*crp* and Δ*opaR* were functionally complemented with their respective gene. The
316 Δ*opaR* pBAD*opaR* showed restoration of CPS and Δ*crp* pBAD*crp* produced a large non-
317 translucent colony (**Fig. 9A**). The Δ*opaR* pBAD*crp* strain remained translucent,

318 suggesting that *crp* cannot rescue the Δ*opaR* CPS defect (**Fig. 9A**). Also, the Δ*crp*
319 pABAD*opaR* mutant did not appear to restore CPS (**Fig. 9A**), however in biofilm assays,
320 Δ*crp* pBAD*crp* produced significantly more biofilm than Δ*crp* pBADEV (**Fig. 9B, Fig.**
321 **9C**). In the Δ*crp* pBAD*opaR* strain, significantly more biofilm was produced compared to
322 Δ*crp* pBADEV, but not to the same level as Δ*crp* pBAD*crp* **(Fig. 9D)**. These data suggest
323 that CRP is epistatic to OpaR in the biofilm regulatory network, but additional factors
324 are involved in biofilm regulation, which needs to be examined further.

325 **DISCUSSION**

326 In this study, the physiological roles of CRP and adenylate cyclase were examined in *V.*
327 *parahaemolyticus*, which led to the identification of an uncharacterized AC-IV named
328 CyaB. The data showed that in *V. parahaemolyticus,* CRP was an important regulator of
329 metabolism and motility, acting as a positive regulator of both swimming and
330 swarming motility. In addition, the data showed that CRP was required for capsule and
331 biofilm formation. In *E. coli* and other enterobacteria deleting *cyaA,* which encodes the
332 canonical AC-I, results in CRP remaining inactive. Thus in these species, the Δ*cyaA* and
333 Δ*crp* mutants have similar phenotypes (51, 52). In *V. cholerae* and *V. vulnificus,* deletion
334 of *cyaA* also gave phenotypes similar to Δ*crp,* showing defects in metabolism and
335 motility (38, 53, 54). In *V. parahaemolyticus,* the Δ*cyaA* mutant showed phenotypes
336 similar to wild type. This unexpected finding led us to search for proteins with putative
337 AC function in the *V. parahaemolyticus* genome leading to the identification of the *cyaB*

338 gene (VP1760). CyaB belongs to the CYTH protein superfamily (Pfam PF01928) and was
339 annotated as a class AC-IV, which contained one domain and was homologous to AC-
340 IV proteins previously described in *A. hydrophila*, *Y. pestis,* and thermophilic
341 archaebacteria (31-34). Our phylogenetic analysis showed that CyaB is widespread
342 throughout the *Vibrionaceae* family generally present in all strains of each species.
343 Several instances of horizontal gene transfer of *cyaB* were noted. Overall, AC-IV
344 homologs were present predominantly among Gamma-Proteobacteria in species
345 belonging to the genera *Aeromonas, Shewanella, Yersinia, Proteus, Providencia, Dickeya,*
346 and *Pectobacterium,* amongst others. In these genera, the CyaB phylogeny usually
347 followed evolutionary relationships, but some *Shewanella* species for example nested
348 within *Vibrio* CyaB clades suggesting horizontal gene transfer. Homologs were also
349 present in Alpha-Proteobacteria, but only in a handful of genera; *Cohaesibacter, Hoeflea,*
350 *Kangsaoukella, Maritalea, and Pseudovibrio.* Outside of Bacteria, proteins annotated as AC-
351 IV were present in Planctomycete, Crenarchaetote and Euryarchaeote species. All
352 bacterial homologs of AC-IV described in this study contained the N-terminal motif
353 HFxxxxExExK. The amino acid residues HF are an important distinguishing feature
354 present in proteins with nucleotidyl cyclase activity, whereas among Planctomycete and
355 Archaea species only the N-terminal motif ExExK is present. Vogt and colleagues recent
356 work showed that archaeal CYTH-like proteins are functionally diverge from bacterial
357 AC-IV CyaB-like proteins (35). They proposed that a true AC-IV requires the extended

358 N-terminal signature HFxxxxExExK, with the HF motif absent in other CYTH proteins
359 that function as either TTM or ThTPase (35).
360 The seminal studies of AC-IV in *A. hydrophila* showed that the protein was only active at
361 high temperatures and alkaline pH conditions (31). Furthermore, their studies showed
362 that deleting *cyaB* did not have any cellular effects under the conditions examined (31).
363 A study in *Shewanella oneidensis* characterized three AC genes, *cyaA, cyaB,* and *cyaC*
364 members of AC-I, AC-IV, and AC-III present in that species. They showed each *cya* gene
365 functionally complemented an *E. coli* Δ*cyaA*, but did not determine any other role for
366 *cyaB* (55). Indeed, to date, no physiological role for AC-IV has been shown. In our study,
367 we show that deleting *cyaB* results in significant defects in metabolism, capsule
368 production, and biofilm formation. The defects in CPS production and biofilm
369 formation in both the Δ*crp* and Δ*cyaB* mutants indicate that cAMP-CRP is a positive
370 regulator of these phenotypes and CyaB is essential for this function. The data may also
371 suggest that cAMP, per se, is not directly involved, but that a function specific to the
372 CYTH superfamily could be.
373 Studies in *V. cholerae* identified cAMP-CRP as a negative regulator of capsule
374 production and biofilm formation (38, 56). It was showed that cAMP-CRP negatively
375 regulated CPS (encoded by *vsp* loci) and biofilm matrix proteins by regulating genes
376 encoding diguanylate cyclases and phosphodiesterases. In *V. cholerae*, the *vsp*
377 biosynthetic operon is negatively controlled by HapR, the quorum sensing master

378 regulator, and it was shown that CRP was epistatic to HapR in the regulation of the
379 VspT and VspR regulators of capsule production (38, 56-59). In these studies both Δ*crp*
380 and Δ*cyaA* showed decreased expression of *hapR* suggesting that cAMP-CRP was a
381 positive regulator of HapR (38, 56, 60). In *V. parahaemolyticus*, the quorum sensing
382 master regulator OpaR is a positive regulator of capsule and biofilm production,
383 however, whether cAMP-CRP controls OpaR is unknown (43, 44, 46-50). Our
384 preliminary bioinformatics analysis identified two putative CRP binding sites in the
385 regulator region of OpaR suggesting CRP may be a direct regulator of *opaR* in *V.*
386 *parahaemolyticus* (**Fig. S12**). Putative CRP binding sites were also identified in *cspA-K*
387 regulator promoter regions, which will need to be investigated further (**Fig. S12**). It is of
388 interest to note that although both *V. cholerae* and *V. parahaemolyticus* use conserved
389 regulatory pathways, QS and CCR, to modulate capsule and biofilm production, the
390 effects are the direct opposite in each species. It will be of interest to determine how this
391 diversity in the control of important phenotypes in these related species has evolved
392 and how CyaB plays a role.
393

394 **MATERIALS AND METHODS**

395 **Bacterial strains, media, and culture conditions.**

396 All strains and plasmids used in this study are listed in **Table 1**. A streptomycin-
397 resistant clinical isolate *V. parahaemolyticus* RIMD2210633 was used throughout the

398 study. Unless stated otherwise, all *V. parahaemolyticus* strains were grown in Luria
399 Bertani (LB) medium (Fischer Scientific, Pittsburgh, PA) containing 3% NaCl (LBS) at
400 37°C with aeration or M9 medium media (Sigma Aldrich, St. Louis, MO) containing 3%
401 NaCl (M9S) supplement with 10mM of various carbon sources. Antibiotics were added
402 to growth media at the following concentrations: Ampicillin (Amp), 100 μg/ml,
403 streptomycin (Sm), 200 μg/ml, chloramphenicol (Cm), 10 μg/ml, and kanamycin (Km),
404 50 μg/ml when required.

405 **Construction of mutant strains in *V. parahaemolyticus* RIMD2210633.**

406 Splice by overlapping extension (SOE) PCR and an allelic exchange (61) was used to
407 construct in-frame, non-polar deletion mutants of *crp* (VP2793), *cyaA* (VP2987), *cyaB*
408 (VP1760) and a double deletion *cyaB*/*cyaA* in *V. parahaemolyticus* RIMD2210633. Primer
409 pairs were designed for *crp* (VP2793), *cyaA* (VP2987), and *cyaB* (VP1760) PCR
410 amplification using *V. parahaemolyticus* RIMD2210633 genomic DNA as a template. All
411 primers used in this study are listed in **Table S1**. Using the PCR amplified fragments of
412 each gene, SOE PCR was conducted to create truncated version of *crp* (leaving 81-bps of
413 633-bp VP2793), *cyaA* (153-bp of 2,529-bp VP2987) and *cyaB* (84-bp of 546-bp VP1760).
414 The truncated PCR fragments were cloned into the suicide vector pDS132 and named
415 pDS*Δcrp*, pDS*ΔcyaA*, and pDS*ΔcyaB*. pDS*Δcrp*, pDS*ΔcyaA*, and pDS*ΔcyaB* were
416 transformed into *E. coli* strain β2155 *λpir*, which were conjugated separately into *V.*
417 *parahaemolyticus*. Conjugation was conducted by spread plating both strains onto LBS

418 plate containing 0.3 mM diaminopimelic acid (DAP). Bacterial growth from this plate
419 was scraped, suspended in LBS, serially diluted, and plated on LBS plates containing
420 streptomycin and chloramphenicol. After overnight growth, colonies were examined to
421 identify single crossovers of the suicide plasmids into the target site via PCR. The
422 colonies with single crossover were grown over night in LBS with no antibiotic and
423 plated onto LBS plate containing 10% sucrose to select for double crossover deletion
424 mutants. The double deletion mutant Δ*cyaB*/Δ*cyaA* was constructed by deleting *cyaA*
425 from Δ*cyaB* background following the above protocol. The gene deletions were
426 confirmed by PCR and DNA sequencing.

427 **Bioinformatics analysis**.

428 The presence of CRP binding sites (BS) in the regulatory regions of *crp, cyaA* and *cyaB* in
429 *V. parahaemolyticus* were examined using PRODORIC software using both the *E. coli* and
430 *V. cholerae* consensus sequences for Crp (62). WebLogo was used to generate graphical
431 representations of the multiple sequence alignments used to generate phylogenetic trees
432 for CyaB (63). Each single letter symbol is the single letter designation of an amino acid
433 at each position in the protein. The height of the each stack for each position indicates
434 the sequence conservation at that position and the height of each symbol within a stack
435 represent the frequency of each amino acid at that position.

436 **Functional complementation of *E. coli* Δ*cyaA* and *V. parahaemolyticus* mutants.**

437 Primer pairs were designed to amplify *cyaA* (VP2987) and *cyaB* (VP1760) using wild
438 type genomic DNA as template (**Table S1**). Purified PCR products of *cyaA* or *cyaB*, and
439 the vector pBBR1MCS were digested using BamHI and XbaI. Both the insert and the
440 vector were gel purified. The genes were each cloned into the vector pBBR1MCS
441 creating pBBR*cyaA* or pBBR*cyaB*, which were then transformed into *E. coli* B2155 using
442 the calcium chloride transformation method. *E. coli* β2155 containing pBBR*cyaA* and
443 pBBR*cyaB* were transformed into *E. coli* Δ*cyaA* and grown overnight in media
444 supplemented with 100 mM isopropyl-β-d-thiogalactopyranoside (IPTG) (64). For
445 functional complementation of *V. parahaemolyticus* Δ*crp*, Δ*cyaB* and Δ*opaR* a similar
446 approach was used, but *crp* and *opaR* as well as *cyaB* were cloned into pBAD33.
447 Complement strains were verified using PCR and sequencing.
448 **Growth pattern analysis.**
449 Bacterial cultures were grown overnight in LBS or M9S supplemented with 10mM
450 glucose at 37°C with aeration. An overnight growth culture was spun down,
451 resuspended, and washed with PBS and a 1: 40 dilution was then used to conduct
452 growth pattern analysis in M9S supplemented with 10 mM of each individual carbon
453 sources. Growth curves were performed in a 96 well plate at 37°C with aeration. Optical
454 density (OD595) was measured each hour for 24 hours. Each experiment was performed
455 in triplicate with two biological replications.
456 **Swimming and swarming motility assay.**

457 Swimming assays were performed in semi-solid media, LB 2% NaCl with 0.3% agar and
458 swarming assays were performed in heart infusion (HI) medium (Remel, Lenexa, KS)
459 containing 2% NaCl and 1.5 % agar. To examine swimming behavior, a single colony of
460 the test bacterium was picked and stabbed in the center of the LB plate and incubated at
461 37°C for 24 h. For the swarming assay, a single colony was picked and gently inoculated
462 on the surface of the HI plate, and the plates were incubated at 30°C for 48 h. Each
463 experiment was performed in triplicate with three biological replications.

464 **Capsule polysaccharide and biofilm production assay.**

465 Capsule polysaccharide (CPS) formation assays were conducted as previously
466 described (43-45). Wild type and mutant strains were grown on HI media containing
467 1.5% agar, 2% NaCl, 2.5 mM $CaCl_2$, and 0.25% Congo red dye for 48 h at 30°C. Each
468 image is an example from at least three biological replicates performed in triplicate.
469 Biofilm assays were performed as previously described (43-45). Briefly, overnight
470 cultures were used to inoculate strip wells in a 1:40 dilution in LBS. Cultures were
471 incubated for 24 h at 37°C prior to analysis. Biofilm was stained with crystal violet and
472 solubilized with dimethyl sulfoxide (DMSO) (ThermoFisher Scientific, USA). Optical
473 density was measured at 595nm to quantify biofilm.

474 **Phylogenetic analysis of AC-IV.**

475 pBLAST searches with VP1760 from *V. parahaemolyticus* used as a seed were performed
476 on all completed and draft genomes published on the National Center for

477 Biotechnology Institute (NCBI) website. Sequences were aligned using CLUSTALW
478 (65). The evolutionary history was inferred by using the Maximum Likelihood method
479 and Kimura 2-parameter model (66). The *cyaB* gene tree with the highest log likelihood
480 (-16932.68) is shown. The percentage of trees in which the associated taxa clustered
481 together is shown next to the branches. A discrete Gamma distribution was used to
482 model evolutionary rate differences among sites (3 categories (+*G*, parameter = 0.5711)).
483 This analysis involved 61 nucleotide sequences. Codon positions included were
484 1st+2nd+3rd. There were a total of 543 positions in the final dataset. The CyaB tree was
485 inferred by using the Maximum Likelihood method and Le_Gascuel_2008 model. The
486 tree with the highest log likelihood (-21377.64) is shown. A discrete Gamma distribution
487 was used to model evolutionary rate differences among sites (3 categories (+*G*,
488 parameter = 0.7213)). This analysis involved 177 amino acid sequences and a total of 145
489 positions in the final dataset. Initial tree(s) for the heuristic search were obtained
490 automatically by applying Neighbor-Join and BioNJ algorithms to a matrix of pairwise
491 distances estimated, and then selecting the topology with superior log likelihood value.
492 Trees are drawn to scale, with branch lengths measured in the number of substitutions
493 per site. All positions with less than 95% site coverage were eliminated, i.e., fewer than
494 5% alignment gaps, missing data, and ambiguous bases were allowed at any position
495 (partial deletion option). Phylogenetic analyses were conducted with MEGA X (67). For
496 the *Vibrio* species that contained CyaB, a second tree was constructed for the same set of

species based on CyaA protein sequences and compared with the CyaA tree to examine differences in branching patterns amongst species.

ACKNOWLEDGMENTS

This research was supported in part by a National Science Foundation grant (award IOS-1656688) to E.F.B. J.G.T was funded by a University of Delaware graduate fellowship award.

503 **REFERENCES:**

504 1. Botsford JL, Harman JG. 1992. Cyclic AMP in prokaryotes. Microbiol Rev 56:100-
505 22.

506 2. Görke B, Stülke J. 2008. Carbon catabolite repression in bacteria: many ways to
507 make the most out of nutrients. Nature Reviews Microbiology 6:613-624.

508 3. Deutscher J. 2008. The mechanisms of carbon catabolite repression in bacteria.
509 Curr Opin Microbiol 11:87-93.

510 4. Deutscher J, Francke C, Postma PW. 2006. How phosphotransferase system-
511 related protein phosphorylation regulates carbohydrate metabolism in bacteria.
512 Microbiol Mol Biol Rev 70:939-1031.

513 5. Danchin A, Guiso N, Roy A, Ullmann A. 1984. Identification of the *Escherichia coli*
514 cya gene product as authentic adenylate cyclase. J Mol Biol 175:403-8.

515 6. Dumay V, Danchin A, Crasnier M. 1996. Regulation of *Escherichia coli* adenylate
516 cyclase activity during hexose phosphate transport. Microbiology (Reading) 142 (
517 Pt 3):575-583.

518 7. Makman RS, Sutherland EW. 1965. Adenosine 3',5'-Phosphate in *Escherichia coli*. J
519 Biol Chem 240:1309-14.

520 8. Stülke J, Hillen W. 1999. Carbon catabolite repression in bacteria. Curr Opin
521 Microbiol 2:195-201.

522 9. Kolb A, Busby S, Buc H, Garges S, Adhya S. 1993. Transcriptional regulation by
523 cAMP and its receptor protein. Annu Rev Biochem 62:749-95.
524 10. Zheng D, Constantinidou C, Hobman JL, Minchin SD. 2004. Identification of the
525 CRP regulon using in vitro and in vivo transcriptional profiling. Nucleic Acids
526 Res 32:5874-93.
527 11. Roy A, Danchin A. 1982. The cya locus of *Escherichia coli* K12: organization and
528 gene products. Mol Gen Genet 188:465-71.
529 12. Roy A, Danchin A, Joseph E, Ullmann A. 1983. Two functional domains in
530 adenylate cyclase of *Escherichia coli*. J Mol Biol 165:197-202.
531 13. Berg OG, von Hippel PH. 1988. Selection of DNA binding sites by regulatory
532 proteins. II. The binding specificity of cyclic AMP receptor protein to recognition
533 sites. J Mol Biol 200:709-23.
534 14. Benoff B, Yang H, Lawson CL, Parkinson G, Liu J, Blatter E, Ebright YW, Berman
535 HM, Ebright RH. 2002. Structural basis of transcription activation: the CAP-alpha
536 CTD-DNA complex. Science 297:1562-6.
537 15. Nelson SO, Wright JK, Postma PW. 1983. The mechanism of inducer exclusion.
538 Direct interaction between purified III of the phosphoenolpyruvate:sugar
539 phosphotransferase system and the lactose carrier of *Escherichia coli*. EMBO J
540 2:715-20.

541 16. Inada T, Kimata K, Aiba H. 1996. Mechanism responsible for glucose-lactose
542 diauxie in *Escherichia coli*: challenge to the cAMP model. Genes Cells 1:293-301.
543 17. Hogema BM, Arents JC, Bader R, Eijkemans K, Yoshida H, Takahashi H, Aiba H,
544 Postma PW. 1998. Inducer exclusion in *Escherichia coli* by non-PTS substrates: the
545 role of the PEP to pyruvate ratio in determining the phosphorylation state of
546 enzyme IIAGlc. Mol Microbiol 30:487-98.
547 18. Saier MH, Jr., Feucht BU, Hofstadter LJ. 1976. Regulation of carbohydrate uptake
548 and adenylate cyclase activity mediated by the enzymes II of the
549 phosphoenolpyruvate: sugar phosphotransferase system in *Escherichia coli*. J Biol
550 Chem 251:883-92.
551 19. Ullmann A, Tillier F, Monod J. 1976. Catabolite modulator factor: a possible
552 mediator of catabolite repression in bacteria. Proc Natl Acad Sci U S A 73:3476-9.
553 20. Danchin A, Dondon L, Daniel J. 1984. Metabolic alterations mediated by 2-
554 ketobutyrate in *Escherichia coli* K12. Mol Gen Genetics 193:473-478.
555 21. You C, Okano H, Hui S, Zhang Z, Kim M, Gunderson CW, Wang YP, Lenz P,
556 Yan D, Hwa T. 2013. Coordination of bacterial proteome with metabolism by
557 cyclic AMP signalling. Nature 500:301-6.
558 22. Bârzu O, Danchin A. 1994. Adenylyl cyclases: a heterogeneous class of ATP-
559 utilizing enzymes. Prog Nucleic Acid Res Mol Biol 49:241-83.

560 23. Ramakrishnan G, Jain A, Chandra N, Srinivasan N. 2016. Computational
561 recognition and analysis of hitherto uncharacterized nucleotide cyclase-like
562 proteins in bacteria. Biol Direct 11:27.
563 24. Crasnier M, Dumay V, Danchin A. 1994. The catalytic domain of *Escherichia coli*
564 K-12 adenylate cyclase as revealed by deletion analysis of the cya gene. Mol Gen
565 Genet 243:409-16.
566 25. Ladant D, Ullmann A. 1999. Bordatella pertussis adenylate cyclase: a toxin with
567 multiple talents. Trends Microbiol 7:172-6.
568 26. Sinha SC, Sprang SR. 2006. Structures, mechanism, regulation and evolution of
569 class III nucleotidyl cyclases. Rev Physiol Biochem Pharmacol 157:105-40.
570 27. Cotta MA, Whitehead TR, Wheeler MB. 1998. Identification of a novel adenylate
571 cyclase in the ruminal anaerobe, Prevotella ruminicola D31d. FEMS Microbiol
572 Lett 164:257-60.
573 28. Téllez-Sosa J, Soberón N, Vega-Segura A, Torres-Márquez ME, Cevallos MA.
574 2002. The Rhizobium etli cyaC product: characterization of a novel adenylate
575 cyclase class. J Bacteriol 184:3560-8.
576 29. Iyer LM, Aravind L. 2002. The catalytic domains of thiamine triphosphatase and
577 CyaB-like adenylyl cyclase define a novel superfamily of domains that bind
578 organic phosphates. BMC Genomics 3:33.

579 30. Martinez J, Truffault V, Hothorn M. 2015. Structural Determinants for Substrate
580 Binding and Catalysis in Triphosphate Tunnel Metalloenzymes. J Biol Chem
581 290:23348-60.
582 31. Sismeiro O, Trotot P, Biville F, Vivares C, Danchin A. 1998. Aeromonas
583 hydrophila adenylyl cyclase 2: a new class of adenylyl cyclases with thermophilic
584 properties and sequence similarities to proteins from hyperthermophilic
585 archaebacteria. J Bacteriol 180:3339-44.
586 32. Gallagher DT, Kim SK, Robinson H, Reddy PT. 2011. Active-site structure of
587 class IV adenylyl cyclase and transphyletic mechanism. J Mol Biol 405:787-803.
588 33. Gallagher DT, Smith NN, Kim SK, Heroux A, Robinson H, Reddy PT. 2006.
589 Structure of the class IV adenylyl cyclase reveals a novel fold. J Mol Biol 362:114-
590 22.
591 34. Smith N, Kim SK, Reddy PT, Gallagher DT. 2006. Crystallization of the class IV
592 adenylyl cyclase from Yersinia pestis. Acta Crystallogr Sect F Struct Biol Cryst
593 Commun 62:200-4.
594 35. Vogt MS, Ngouoko Nguepbeu RR, Mohr MKF, Albers SV, Essen LO, Banerjee A.
595 2021. The archaeal triphosphate tunnel metalloenzyme SaTTM defines structural
596 determinants for the diverse activities in the CYTH protein family. J Biol Chem
597 297:100820.

598 36. Kovacikova G, Skorupski K. 2001. Overlapping binding sites for the virulence
599 gene regulators AphA, AphB and cAMP-CRP at the *Vibrio cholerae* tcpPH
600 promoter. Mol Microbiol 41:393-407.
601 37. Li CC, Merrell DS, Camilli A, Kaper JB. 2002. ToxR interferes with CRP-
602 dependent transcriptional activation of ompT in *Vibrio cholerae*. Mol Microbiol
603 43:1577-89.
604 38. Liang W, Pascual-Montano A, Silva AJ, Benitez JA. 2007. The cyclic AMP
605 receptor protein modulates quorum sensing, motility and multiple genes that
606 affect intestinal colonization in *Vibrio cholerae*. Microbiology (Reading) 153:2964-
607 2975.
608 39. Popovych N, Tzeng SR, Tonelli M, Ebright RH, Kalodimos CG. 2009. Structural
609 basis for cAMP-mediated allosteric control of the catabolite activator protein.
610 Proc Natl Acad Sci U S A 106:6927-32.
611 40. Shimada T, Fujita N, Yamamoto K, Ishihama A. 2011. Novel roles of cAMP
612 receptor protein (CRP) in regulation of transport and metabolism of carbon
613 sources. PLoS One 6:e20081.
614 41. Skorupski K, Taylor RK. 1997. Cyclic AMP and its receptor protein negatively
615 regulate the coordinate expression of cholera toxin and toxin-coregulated pilus in
616 *Vibrio cholerae*. Proc Natl Acad Sci U S A 94:265-70.

617 42. Whitaker WB, Richards GP, Boyd EF. 2014. Loss of sigma factor RpoN increases
618 intestinal colonization of *Vibrio parahaemolyticus* in an adult mouse model. Infect
619 Immun 82:544-56.
620 43. Kalburge SS, Carpenter MR, Rozovsky S, Boyd EF. 2017. Quorum Sensing
621 Regulators Are Required for Metabolic Fitness in *Vibrio parahaemolyticus*. Infect
622 Immun 85.
623 44. Tague JG, Hong J, Kalburge SS, Boyd EF. 2022. Regulatory Small RNA Qrr2 Is
624 Expressed Independently of Sigma Factor-54 and Can Function as the Sole Qrr
625 Small RNA To Control Quorum Sensing in *Vibrio parahaemolyticus*. J Bacteriol
626 204:e0035021.
627 45. Tague JG, Regmi A, Gregory GJ, Boyd EF. 2021. Fis Connects Two Sensory
628 Pathways, Quorum Sensing and Surface Sensing, to Control Motility in *Vibrio*
629 *parahaemolyticus*. Front Microbiol 12:669447.
630 46. McCarter LL. 1998. OpaR, a homolog of Vibrio harveyi LuxR, controls opacity of
631 *Vibrio parahaemolyticus*. J Bacteriol 180:3166-73.
632 47. Guvener ZT, McCarter LL. 2003. Multiple regulators control capsular
633 polysaccharide production in *Vibrio parahaemolyticus*. J Bacteriol 185:5431-41.
634 48. Enos-Berlage JL, Guvener ZT, Keenan CE, McCarter LL. 2005. Genetic
635 determinants of biofilm development of opaque and translucent *Vibrio*
636 *parahaemolyticus*. Mol Microbiol 55:1160-82.

637 49. Kernell Burke A, Guthrie LT, Modise T, Cormier G, Jensen RV, McCarter LL,
638 Stevens AM. 2015. OpaR controls a network of downstream transcription factors
639 in *Vibrio parahaemolyticus* BB22OP. PLoS One 10:e0121863.
640 50. Gode-Potratz CJ, McCarter LL. 2011. Quorum sensing and silencing in *Vibrio*
641 *parahaemolyticus*. J Bacteriol 193:4224-37.
642 51. Hufnagel DA, Evans ML, Greene SE, Pinkner JS, Hultgren SJ, Chapman MR.
643 2016. The Catabolite Repressor Protein-Cyclic AMP Complex Regulates csgD and
644 Biofilm Formation in Uropathogenic *Escherichia coli*. J Bacteriol 198:3329-3334.
645 52. Kalivoda EJ, Stella NA, O'Dee DM, Nau GJ, Shanks RM. 2008. The cyclic AMP-
646 dependent catabolite repression system of Serratia marcescens mediates biofilm
647 formation through regulation of type 1 fimbriae. Appl Environ Microbiol
648 74:3461-70.
649 53. Kim YR, Kim SY, Kim CM, Lee SE, Rhee JH. 2005. Essential role of an adenylate
650 cyclase in regulating *Vibrio vulnificus* virulence. FEMS Microbiol Lett 243:497-503.
651 54. Kim YR, Lee SE, Kim B, Choy H, Rhee JH. 2013. A dual regulatory role of cyclic
652 adenosine monophosphate receptor protein in various virulence traits of *Vibrio*
653 *vulnificus*. Microbiol Immunol 57:273-80.
654 55. Charania MA, Brockman KL, Zhang Y, Banerjee A, Pinchuk GE, Fredrickson JK,
655 Beliaev AS, Saffarini DA. 2009. Involvement of a membrane-bound class III

656 adenylate cyclase in regulation of anaerobic respiration in *Shewanella oneidensis*
657 MR-1. J Bacteriol 191:4298-306.
658 56. Fong JCN, Yildiz FH. 2008. Interplay between Cyclic AMP-Cyclic AMP Receptor
659 Protein and Cyclic di-GMP Signaling in *Vibrio cholerae* Biofilm Formation. J
660 Bacteriol 190:6646-6659.
661 57. Hammer BK, Bassler BL. 2003. Quorum sensing controls biofilm formation in
662 *Vibrio cholerae*. Mol Microbiol 50:101-4.
663 58. Zhu J, Mekalanos JJ. 2003. Quorum sensing-dependent biofilms enhance
664 colonization in *Vibrio cholerae*. Dev Cell 5:647-56.
665 59. Yildiz FH, Liu XS, Heydorn A, Schoolnik GK. 2004. Molecular analysis of
666 rugosity in a *Vibrio cholerae* O1 El Tor phase variant. Mol Microbiol 53:497-515.
667 60. Silva AJ, Pham K, Benitez JA. 2003. Haemagglutinin/protease expression and
668 mucin gel penetration in El Tor biotype *Vibrio cholerae*. Microbiology 149:1883-
669 1891.
670 61. Ho SN, Hunt HD, Horton RM, Pullen JK, Pease LR. 1989. Site-directed
671 mutagenesis by overlap extension using the polymerase chain reaction. Gene
672 77:51-9.
673 62. Grote A, Klein J, Retter I, Haddad I, Behling S, Bunk B, Biegler I, Yarmolinetz S,
674 Jahn D, Münch R. 2009. PRODORIC (release 2009): a database and tool platform
675 for the analysis of gene regulation in prokaryotes. Nucleic Acids Res 37:D61-5.

676 63. Crooks GE, Hon G, Chandonia JM, Brenner SE. 2004. WebLogo: a sequence logo
677 generator. Genome Res 14:1188-90.
678 64. Baba T, Ara T, Hasegawa M, Takai Y, Okumura Y, Baba M, Datsenko KA, Tomita
679 M, Wanner BL, Mori H. 2006. Construction of *Escherichia coli* K-12 in-frame,
680 single-gene knockout mutants: the Keio collection. Mol Syst Biol 2:2006.0008.
681 65. Thompson JD, Higgins DG, Gibson TJ. 1994. CLUSTAL W: improving the
682 sensitivity of progressive multiple sequence alignment through sequence
683 weighting, position-specific gap penalties and weight matrix choice. Nucleic
684 Acids Res 22:4673-80.
685 66. Kimura M. 1980. A simple method for estimating evolutionary rates of base
686 substitutions through comparative studies of nucleotide sequences. J Mol Evol
687 16:111-20.
688 67. Kumar S, Stecher G, Li M, Knyaz C, Tamura K. 2018. MEGA X: Molecular
689 Evolutionary Genetics Analysis across Computing Platforms. Mol Biol Evol
690 35:1547-1549.
691 68. Makino K, Oshima K, Kurokawa K, Yokoyama K, Uda T, Tagomori K, Iijima Y,
692 Najima M, Nakano M, Yamashita A, Kubota Y, Kimura S, Yasunaga T, Honda T,
693 Shinagawa H, Hattori M, Iida T. 2003. Genome sequence of *Vibrio*
694 *parahaemolyticus*: a pathogenic mechanism distinct from that of *V. cholerae*. Lancet
695 361:743-9.

696 69. Baba T, Ara T, Hasegawa M, Takai Y, Okumura Y, Baba M, Datsenko KA, Tomita
697 M, Wanner BL, Mori H. 2006. Construction of *Escherichia coli* K-12 in-frame,
698 single-gene knockout mutants: the Keio collection. Mol Syst Biol 2:2006 0008.
699 70. Dehio C, Meyer M. 1997. Maintenance of broad-host-range incompatibility group
700 P and group Q plasmids and transposition of Tn5 in Bartonella henselae
701 following conjugal plasmid transfer from *Escherichia coli*. J Bacteriol 179:538-40.
702 71. Philippe N, Alcaraz J, Coursange E, Geiselmann J, Schneider D. 1994.
703 Improvement of pCVD442, a suicide plasmid for gene allele exchange in bacteria.
704 Plasmid 51:246-255.
705 72. Kovach ME, Phillips RW, Elzer PH, Roop RM, Peterson KM. 1994. pBBR1MCS: a
706 broad-host-range cloning vector. Biotechniques 16:800-802.
707 73. Guzman LM, Belin D, Carson MJ, Beckwith J. 1995. Tight regulation, modulation,
708 and high-level expression by vectors containing the arabinose PBAD promoter. J
709 Bacteriol 177:4121-30.
710

711 **Figure Legends**

712 **Fig. 1. Growth pattern analysis in LBS and M9S D-Glucose.** Growth pattern analysis
713 of *V. parahaemolyticus* RIMD2210633 (WT), Δ*cyaA*, Δ*cyaB*, Δ*cyaB*/Δ*cyaA,* and Δ*crp* in **(A)**
714 LBS **(B)** M9S + 10mM D-glucose grown at 37°C with aeration for 24 h. For growth in M9,
715 the strains were grown overnight in M9 3%NaCl (M9S) + 10mM glucose (M9GS) at 37°C
716 with aeration for 24 h. Optical density (OD_{595}) was measured every hour for 24 h; means
717 and standard errors of at least two biological replicates are displayed. For all growth
718 curves the area under curve (AUC) was calculated for each strain and a Student's *t*-test
719 was performed, *P<0.05; *** *P*<0.001.

720 **Fig. 2. Growth pattern analysis in alternative carbon sources.** Growth pattern analysis
721 of *V. parahaemolyticus* RIMD2210633 (WT), Δ*cyaA*, Δ*cyaB*, Δ*cyaB*/Δ*cyaA,* and Δ*crp* in **(A)**
722 M9S + 10mM L-arabinose, **(B)** M9S + 10mM L-ribose **(C)** M9S + 10mM D-gluconate at
723 37°C with aeration for 24 h. Inoculums were grown overnight in M9S + 10mM glucose
724 at 37°C with aeration. Optical density (OD_{595}) was measured every hour for 24 h; means
725 and standard errors of at least two biological replicates are displayed. For all growth
726 curves the area under curve (AUC) was calculated for each strain and a Student's *t*-test
727 was performed, ** P<0.01; *** *P*<0.001.

728 **Fig. 3. Evolutionary analysis by of *cyaB* among the family *Vibrionaceae*.** Phylogenetic
729 analysis was conducted in MEGA X. The evolutionary history was inferred by using the
730 Maximum Likelihood method and Kimura 2-parameter model. The *cyaB* gene tree with

731 the highest log likelihood (-16932.68) is shown. The percentage of trees in which the
732 associated taxa clustered together is shown next to the branches. This analysis involved
733 61 nucleotide sequences and a total of 543 positions in the final dataset.

734 **Fig. 4. Evolutionary analysis by of CyaB among Gamma- Proteobacteria, Alpha-**
735 **Proteobacteria, Planctomycete and Archaea species**. The CyaB tree was inferred by
736 using the Maximum Likelihood method and Le_Gascuel_2008 model. The tree with the
737 highest log likelihood (-21377.64) is shown. This analysis involved 177 amino acid
738 sequences and a total of 145 positions in the final dataset.

739 **Fig. 5: Complementation analysis of *E. coli* Δ*cyaA*.** The *E. coli* Δ*cyaA* strain was
740 complemented with a functional copy of *cyaA* or *cyaB* from *V. parahaemolyticus* and
741 growth curves were conducted in **(A)** M9 + 10 mM glucose **(B)** M9 + 10mM gluconate
742 for 48 h at 37°C with aeration. Optical density (OD_{595}) was measured every hour for
743 24 h; means and standard errors of three biological replicates are displayed. For all
744 growth curves the area under curve (AUC) was calculated for each strain and a
745 Student's *t*-test was performed, ** $P<0.01$.

746 **Fig. 6. Characterization of motility in *V. parahaemolyticus* mutants. (A)** Swimming
747 assays were conducted using wild type, Δ*crp*, Δ*cyaA*, Δ*cyaB*, and Δ*cyaB*/Δ*cyaA* mutants
748 grown at 37°C for 24 h in LB 2% NaCl with 0.3% agar. The diameter of the region
749 covered by the bacterial strains were measured and represented as bar graph. The error
750 bars indicate standard error of mean and an Unpaired Student t-test was conducted.

751 The significant difference is denoted by asterisks ***, P<0.001 and NS indicates not

752 significant **(B)** Swarming assays. Colonies of wild type and mutant strains Δ*crp*, Δ*cyaA*,

753 Δ*cyaB*, and Δ*cyaB*/Δ*cyaA* were assessed for swarming motility in HI containing 2% NaCl

754 and 1.5% agar at 30°C for 48 h.

755 **Fig. 7. Capsule polysaccharide production**. Colonies of *V. parahaemolyticus*

756 RIMD2210633 and mutant strains were inoculated on HI plate containing Congo red

757 dye and $CaCl_2$ grown at 37°C for 24 h.

758 **Fig. 8. Biofilm formation**. *V. parahaemolyticus* strains were grown in HI broth for 24 h.

759 **A**. The biofilms were visualized using crystal violet and then dissolved using DMSO,

760 and the optical density of the biofilms were measured at OD and **B.** represented as bar

761 graphs. Error bars indicate standard error of mean (SEM). Unpaired Student *t* test was

762 conducted to obtain the *P* values. The significant difference in biofilm production is

763 denoted by asterisks. *, P<0.05, **, P<0.01, ***, P<0.001. NS, not significant.

764 **Fig. 9. A**. Capsule polysaccharide (CPS) assays. The pBAD*opaR* and pBAD*crp*

765 complementation plasmids were conjugated into *V. parahaemolyticus* mutant strains.

766 Cells were grown on HI congo red $CaCl_2$ media with 0.1% L-arabinose and 12.5 μg/mL

767 chloramphenicol at 30ºC for 48 h prior to imaging. **B.** Biofilm production assays. *V.*

768 *parahaemolyticus* Δ*crp* mutant containing pBAD33 (pBADEV), pBAD*crp*, or pBAD*opaR*

769 expression plasmids were grown in 3% LB with 12.5 μg/mL chloramphenicol and 0.1%

770 L-arabinose for 24 hours at 37˚C. **C.** Biofilm solubilized in DMSO. **D**. Biofilm measured

771 for absorbance at OD_{595}. Error bars indicate standard error of mean (SEM). An Unpaired

772 Student *t* test was conducted to obtain ***, $P<0.001$.

773

774 **Table 1. Bacterial strains and plasmids used in this study**

Bacterial strains	**Genotype or description**	**References or sources**
Vibrio parahaemolyticus		
RIMD2210633	O3:K6 clinical isolate, Sm^r	(68)
Δ*crp*	RIMD2210633 Δ*crp* (VP2793), Sm^r	This study
Δ*cyaA*	RIMD2210633 Δ*cyaA* (VP2987), Sm^r	This study
Δ*cyaB*	RIMD2210633 Δ*cyaB* (VP1760), Sm^r	This study
Δ*cyaB*/Δ*cyaA*	RIMD2210633 Δ*cyaB* Δ*cyaA* (VP2987), Sm^r	This study
Δ*rpoN*	RIMD2210633 Δ*rpoN* (VP2670), Sm^r	(42)
Δ*opaR*	RIMD2210633 Δ*opaR* (VP2516), Sm^r	(43)
Escherichia coli		
BW25113	Wild-Type *E. coli* K12 strain	(69)
Δ*cyaA*	BW25113, F-, *Δ(araD-araB)567, ΔlacZ4787(::rrnB-3), λ⁻, rph-1, ΔcyaA751::kan, Δ(rhaD-rhaB)568, hsdR514*	(69)
DH5αλpir	Δ*lac pir*	Laboratory collection
B2155λpir	*ΔdapA::emr pir*, for bacterial conjugation	(70)
B2155pDS*crp*	B2155 strain harboring pDS*crp*	This study
B2155pDS*cyaA*	B2155 strain harboring pDS*cyaA*	This study
B2155pDS*cyaB*	B2155 strain harboring pDS*cyaB*	This study
Complement strains		This study
E. coli Δ*cyaA*pBBR*cyaA*	*E. coli* Δ*cyaA* harboring pBBR*cyaA*	This study
E. coli Δ*cyaA*pBBR*cyaB*	*E. coli* Δ*cyaA* harboring pBBR*cyaB*	This study
E. coli Δ*cyaA*pBBR*cyaB*	*E. coli* Δ*cyaA* harboring pBBR*cyaB*	This study
V. parahaemolyticus Δ*cyaB*pBBR*cyaB*	*V. parahaemolyticus* Δ*cyaB* harboring pBBR*cyaB*	This study
V. parahaemolyticus Δ*crp*pBAD*crp*	*V. parahaemolyticus* Δ*crp* harboring pBAD*crp*	This study
V. parahaemolyticus Δ*opaR*pBAD*opaR*	*V. parahaemolyticus* Δ*opaR* harboring pBAD*opaR*	This study
V. parahaemolyticus Δ*crp*pBAD*opaR*	*V. parahaemolyticus* Δ*crp* harboring pBAD*opaR*	This study
Plasmids		
pDS132	Suicide plasmid, Cm^r, SacB	(71)
pDSΔ*crp*	pDS132 harboring truncated *crp*, Cm^r	This study

pDSΔ*cyaA*	pDS132 harboring truncated *cyaA*, Cm^r	This study
pDSΔ*cyaB*	pDS132 harboring truncated *cyaB*, Cm^r	This study
pBBR1MCS	Expression vector, P_{LAC} promoter, Cm^r	(72)
pBAD33	Expression vector, P_{BAD} promoter, Cm^r	(73)
pBAD*crp*	pBAD harboring full-length *crp* (VP2793), Cm^r	This study
pBAD*opaR*	pBAD harboring full-length *opaR*, Cm^r	This study
pBBR*cyaA*	pBBR1MCS harboring full-length *cyaA* (VP2987), Cm^r	This study
pBBR*cyaB*	pBBR1MCS harboring full-length *cyaB*(VP1760), Cm^r	This study

775

776

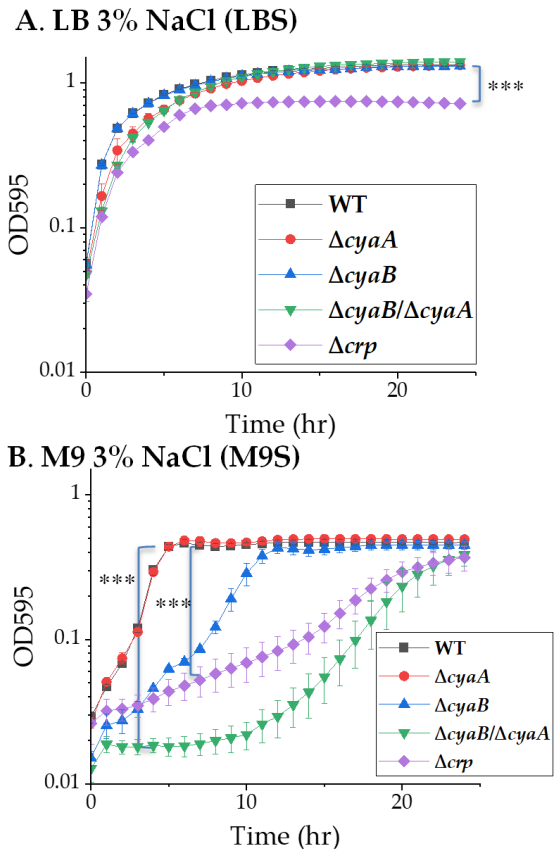
A. LB 3% NaCl (LBS)
OD595
1
0.1
0.01
0
10
20
Time (hr)
***
WT
ΔcyaA
ΔcyaB
ΔcyaB/ΔcyaA
Δcrp
B. M9 3% NaCl (M9S)
OD595
1
0.1
0.01
0
10
20
Time (hr)
***
***
WT
ΔcyaA
ΔcyaB
ΔcyaB/ΔcyaA
Δcrp

Fig. 1

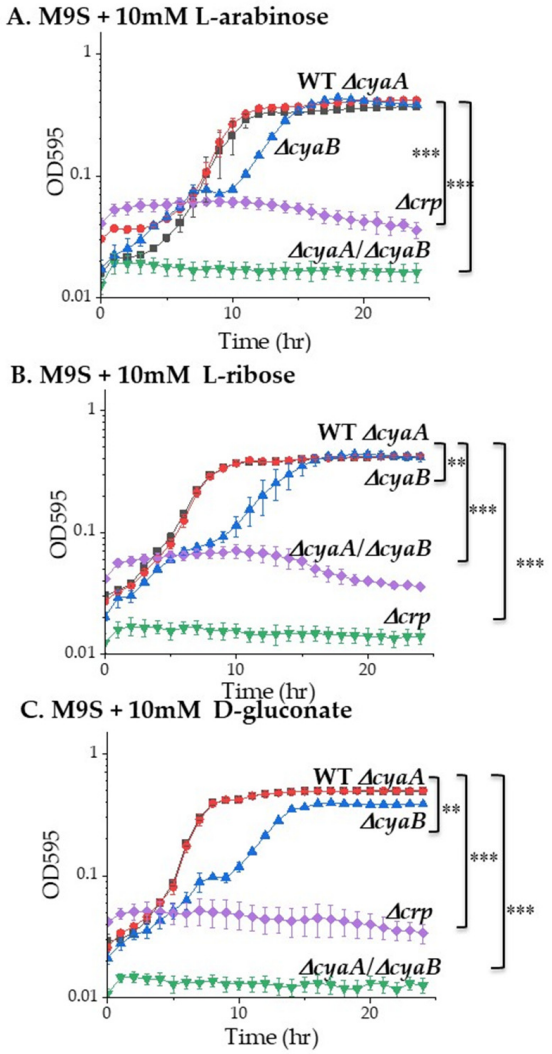
A. M9S + 10mM L-arabinose
WT ΔcyaA
ΔcyaB
Δcrp
ΔcyaA/ΔcyaB
***
***
OD595
1
0.1
0.01
0
10
20
Time (hr)
B. M9S + 10mM L-ribose
WT ΔcyaA
ΔcyaB
ΔcyaA/ΔcyaB
Δcrp
**
***
***
OD595
1
0.1
0.01
0
10
20
Time (hr)
C. M9S + 10mM D-gluconate
WT ΔcyaA
ΔcyaB
Δcrp
ΔcyaA/ΔcyaB
**
***
***
OD595
1
0.1
0.01
0
10
20
Time (hr)

Fig. 2

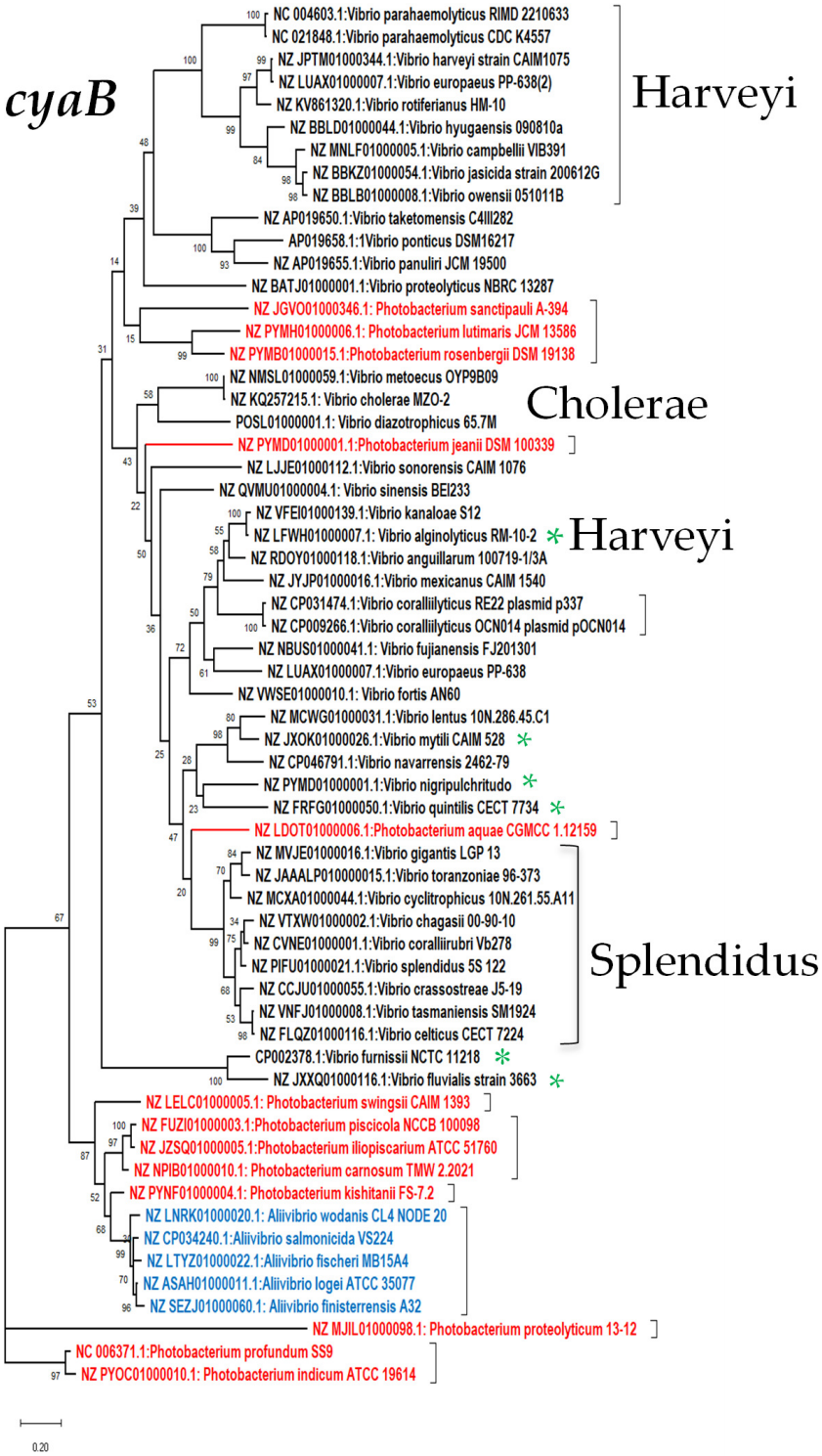
cyaB
Harveyi
NC 004603.1:Vibrio parahaemolyticus RIMD 2210633
NC 021848.1:Vibrio parahaemolyticus CDC K4557
NZ JPTM01000344.1:Vibrio harveyi strain CAIM1075
NZ LUAX01000007.1:Vibrio europaeus PP-638(2)
NZ KV861320.1:Vibrio rotiferianus HM-10
NZ BBLD01000044.1:Vibrio hyugaensis 090810a
NZ MNLF01000005.1:Vibrio campbellii VIB391
NZ BBKZ01000054.1:Vibrio jasicida strain 200612G
NZ BBLB01000008.1:Vibrio owensii 051011B
NZ AP019650.1:Vibrio taketomensis C4III282
AP019658.1:1Vibrio ponticus DSM16217
NZ AP019655.1:Vibrio panuliri JCM 19500
NZ BATJ01000001.1:Vibrio proteolyticus NBRC 13287
NZ JGVO01000346.1: Photobacterium sanctipauli A-394
NZ PYMH01000006.1: Photobacterium lutimaris JCM 13586
NZ PYMB01000015.1:Photobacterium rosenbergii DSM 19138
Cholerae
NZ NMSL01000059.1:Vibrio metoecus OYP9B09
NZ KQ257215.1: Vibrio cholerae MZO-2
POSL01000001.1: Vibrio diazotrophicus 65.7M
NZ PYMD01000001.1:Photobacterium jeanii DSM 100339
NZ LJJE01000112.1:Vibrio sonorensis CAIM 1076
NZ QVMU01000004.1: Vibrio sinensis BEI233
Harveyi
NZ VFEI01000139.1:Vibrio kanaloae S12
NZ LFWH01000007.1: Vibrio alginolyticus RM-10-2
NZ RDOY01000118.1:Vibrio anguillarum 100719-1/3A
NZ JYJP01000016.1:Vibrio mexicanus CAIM 1540
NZ CP031474.1:Vibrio coralliilyticus RE22 plasmid p337
NZ CP009266.1:Vibrio coralliilyticus OCN014 plasmid pOCN014
NZ NBUS01000041.1: Vibrio fujianensis FJ201301
NZ LUAX01000007.1:Vibrio europaeus PP-638
NZ VWSE01000010.1: Vibrio fortis AN60
NZ MCWG01000031.1:Vibrio lentus 10N.286.45.C1
NZ JXOK01000026.1:Vibrio mytili CAIM 528
NZ CP046791.1:Vibrio navarrensis 2462-79
NZ PYMD01000001.1:Vibrio nigripulchritudo
NZ FRFG01000050.1:Vibrio quintilis CECT 7734
NZ LDOT01000006.1:Photobacterium aquae CGMCC 1.12159
Splendidus
NZ MVJE01000016.1:Vibrio gigantis LGP 13
NZ JAAALP010000015.1:Vibrio toranzoniae 96-373
NZ MCXA01000044.1:Vibrio cyclitrophicus 10N.261.55.A11
NZ VTXW01000002.1:Vibrio chagasii 00-90-10
NZ CVNE01000001.1:Vibrio coralliirubri Vb278
NZ PIFU01000021.1:Vibrio splendidus 5S 122
NZ CCJU01000055.1:Vibrio crassostreae J5-19
NZ VNFJ01000008.1:Vibrio tasmaniensis SM1924
NZ FLQZ01000116.1:Vibrio celticus CECT 7224
CP002378.1:Vibrio furnissii NCTC 11218
NZ JXXQ01000116.1:Vibrio fluvialis strain 3663
NZ LELC01000005.1: Photobacterium swingsii CAIM 1393
NZ FUZI01000003.1:Photobacterium piscicola NCCB 100098
NZ JZSQ01000005.1:Photobacterium iliopiscarium ATCC 51760
NZ NPIB01000010.1: Photobacterium carnosum TMW 2.2021
NZ PYNF01000004.1: Photobacterium kishitanii FS-7.2
NZ LNRK01000020.1: Aliivibrio wodanis CL4 NODE 20
NZ CP034240.1:Aliivibrio salmonicida VS224
NZ LTYZ01000022.1:Aliivibrio fischeri MB15A4
NZ ASAH01000011.1:Aliivibrio logei ATCC 35077
NZ SEZJ01000060.1: Aliivibrio finisterrensis A32
NZ MJIL01000098.1: Photobacterium proteolyticum 13-12
NC 006371.1:Photobacterium profundum SS9
NZ PYOC01000010.1: Photobacterium indicum ATCC 19614
0.20

Fig. 3

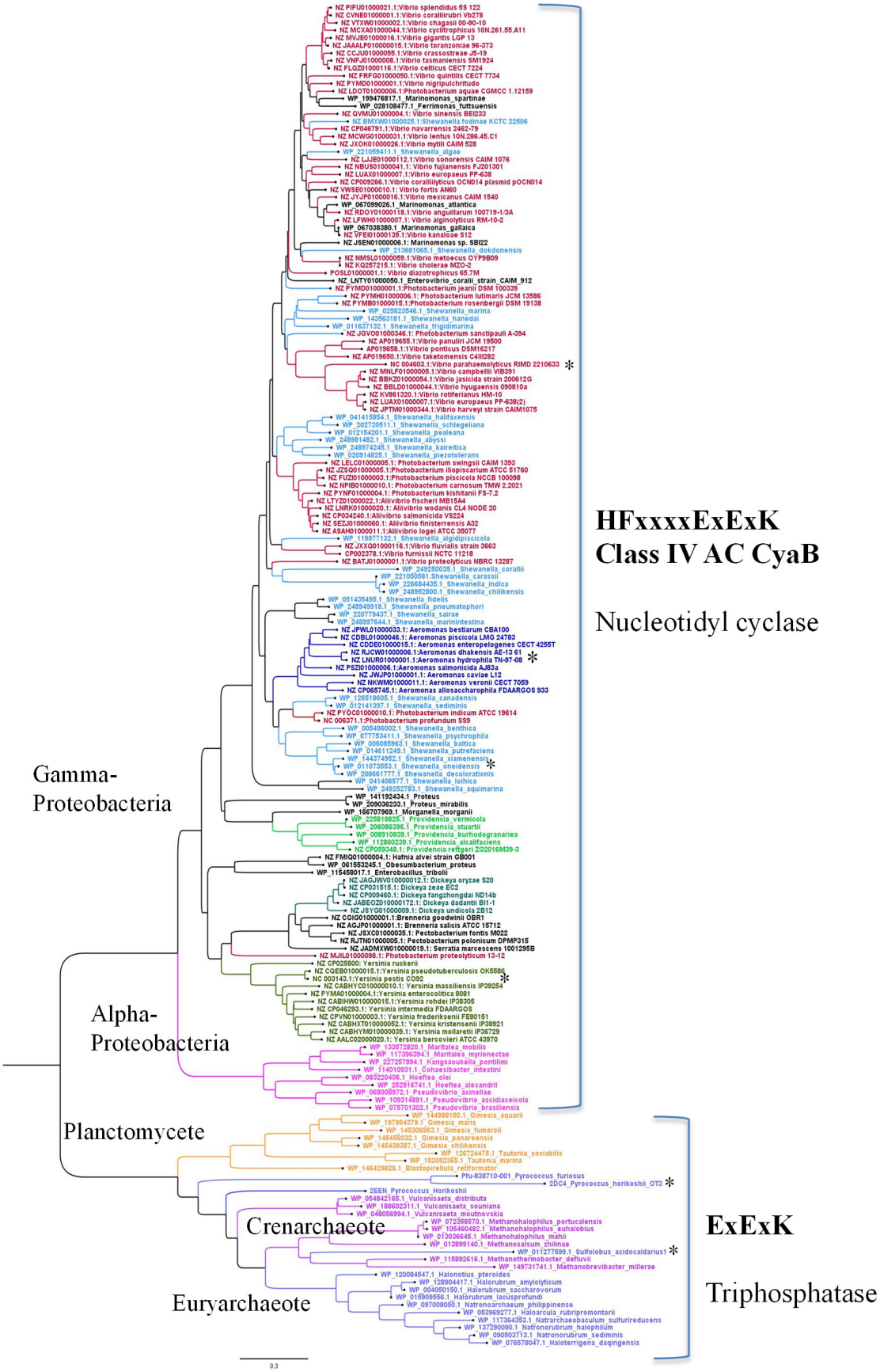
HFxxxxExExK
Class IV AC CyaB
Nucleotidyl cyclase
Gamma-Proteobacteria
Alpha-Proteobacteria
Planctomycete
Crenarchaeote
Euryarchaeote
ExExK
Triphosphatase
0.3

Fig. 4

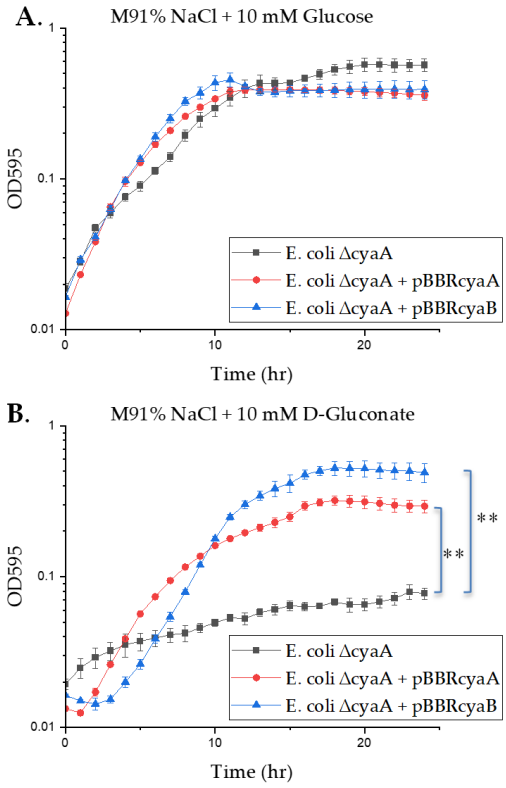
A.
M91% NaCl + 10 mM Glucose
OD595
1
0.1
0.01
0
10
20
Time (hr)
E. coli ΔcyaA
E. coli ΔcyaA + pBBRcyaA
E. coli ΔcyaA + pBBRcyaB
B.
M91% NaCl + 10 mM D-Gluconate
OD595
1
0.1
0.01
0
10
20
Time (hr)
**
**
E. coli ΔcyaA
E. coli ΔcyaA + pBBRcyaA
E. coli ΔcyaA + pBBRcyaB

Fig. 5

A. Swimming motility

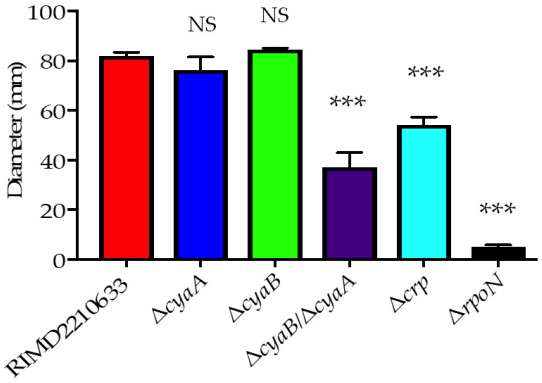

B. Swarming motility

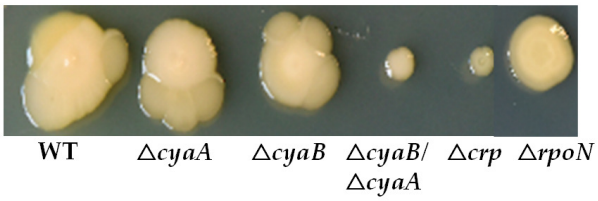

Fig. 6

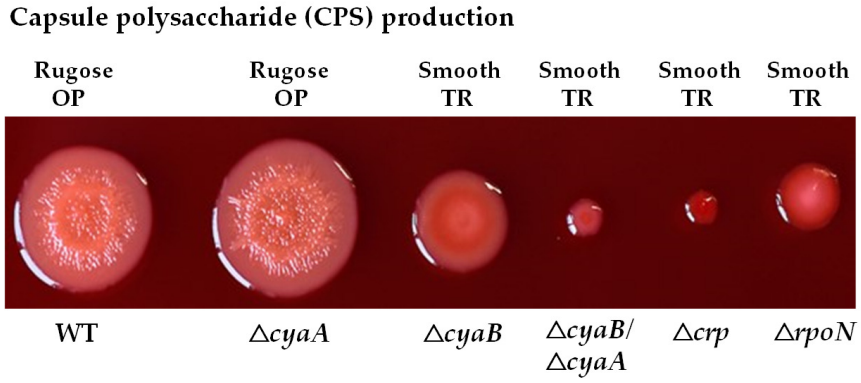
Capsule polysaccharide (CPS) production
Rugose OP
Rugose OP
Smooth TR
Smooth TR
Smooth TR
Smooth TR
WT
△cyaA
△cyaB
△cyaB/ △cyaA
△crp
△rpoN

Fig. 7

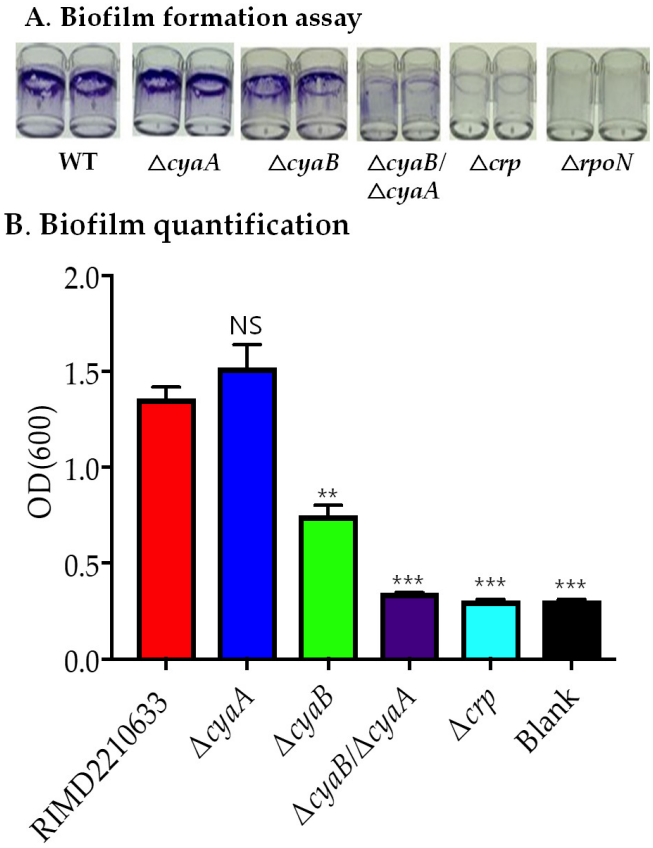
A. Biofilm formation assay
WT
ΔcyaA
ΔcyaB
ΔcyaB/ ΔcyaA
Δcrp
ΔrpoN
B. Biofilm quantification
OD(600)
2.0
1.5
1.0
0.5
0.0
NS
**
***
***
***
RIMD2210633
ΔcyaA
ΔcyaB
ΔcyaB/ΔcyaA
Δcrp
Blank

Fig. 8

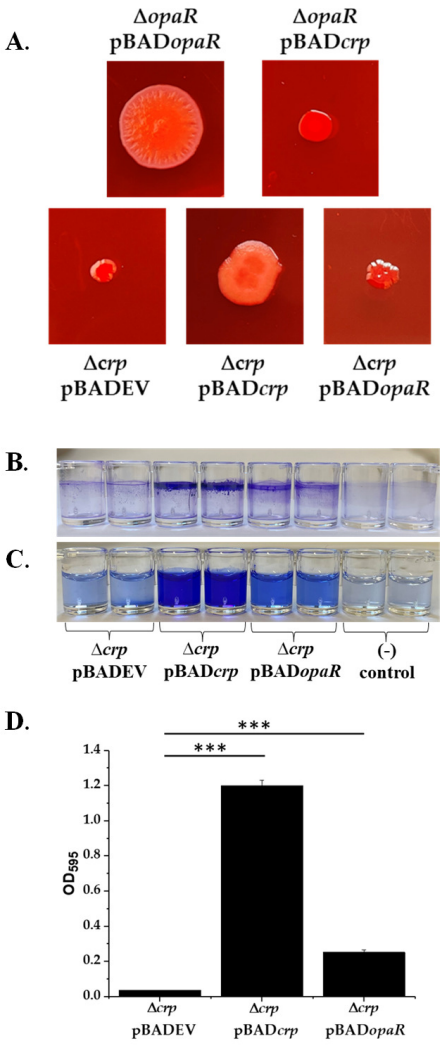
A.
ΔopaR pBADopaR
ΔopaR pBADcrp
Δcrp pBADEV
Δcrp pBADcrp
Δcrp pBADopaR
B.
C.
Δcrp pBADEV
Δcrp pBADcrp
Δcrp pBADopaR
(-) control
D.
***
***
OD595
1.4
1.2
1.0
0.8
0.6
0.4
0.2
0.0
Δcrp pBADEV
Δcrp pBADcrp
Δcrp pBADopaR

Fig. 9.